Clinical Cancer Research

Whole Genomic Copy Number Alterations in Circulating Tumor Cells from Men with Abiraterone or Enzalutamide-Resistant Metastatic Castration-Resistant Prostate Cancer

Santosh Gupta[1,2], Jing Li[3], Gabor Kemeny[1], Rhonda L. Bitting[3], Joshua Beaver[2], Jason A. Somarelli[1], Kathryn E. Ware[1], Simon Gregory[2], and Andrew J. Armstrong[1]

Abstract

Purpose: Beyond enumeration, circulating tumor cells (CTCs) can provide genetic information from metastatic cancer that may facilitate a greater understanding of tumor biology and enable a precision medicine approach.

Experimental Design: CTCs and paired leukocytes from men with metastatic castration-resistant prostate cancer (mCRPC) were isolated from blood through red cell lysis, CD45 depletion, and flow sorting based on EpCAM/CD45 expression. We next performed whole genomic copy number analysis of CTCs and matched patient leukocytes (germline) using array-based comparative genomic hybridization (aCGH) from 16 men with mCRPC, including longitudinal and sequential aCGH analyses of CTCs in the context of enzalutamide therapy.

Results: All patients had mCRPC and primary or acquired resistance to abiraterone acetate or enzalutamide. We compiled copy gains and losses, with a particular focus on those genes highly implicated in mCRPC progression and previously validated as being aberrant in metastatic tissue samples and genomic studies of reference mCRPC datasets. Genomic gains in >25% of CTCs were observed in *AR*, *FOXA1*, *ABL1*, *MET*, *ERG*, *CDK12*, *BRD4*, and *ZFHX3*, while common genomic losses involved *PTEN*, *ZFHX3*, *PDE4DIP*, *RAF1*, and *GATA2*. Analysis of aCGH in a sample with sequential enzalutamide-resistant visceral progression showed acquired loss of *AR* amplification concurrent with gain of *MYCN*, consistent with evolution toward a neuroendocrine-like, AR-independent clone.

Conclusions: Genomic analysis of pooled CTCs in men with mCRPC suggests a reproducible, but highly complex molecular profile that includes common aberrations in *AR*, *ERG*, *c-MET*, and PI3K signaling during mCRPC progression, which may be useful for predictive biomarker development. *Clin Cancer Res; 23(5); 1346–57. ©2016 AACR.*

Introduction

Our understanding of the genomic complexities of metastatic prostate cancer has been greatly accelerated with the advent of next-generation tissue-based sequencing approaches (1–4). These sequencing efforts have revealed significant heterogeneity in genomic lesions across patients with metastatic castration-resistant prostate cancer (mCRPC). Despite this interpatient heterogeneity, a number of key oncogenic pathways are commonly altered, including the androgen receptor (AR), genes in the PI3K pathway, epigenetic pathways, WNT signaling pathway, and DNA repair pathways (1, 2). Interestingly, many of these pathway alterations are potentially actionable and suggest a path forward for developing specific, personalized therapies.

While analysis of metastatic biopsy sites can provide clinically useful information, genomic profiling of a single metastatic site is challenging for several reasons. First, genomic and clonal heterogeneity between metastatic sites within individual patients is known to be prevalent in men with mCRPC (5, 6). Second, metastatic biopsies are invasive, particularly in patients for whom metastases involve bone or visceral sites where sequential biopsies are often not feasible. Third, the yield of evaluable tumor tissue from metastatic sites can often be quite low, particularly from bone metastases (7). Fourth, during therapy-induced clonal selection, dynamic changes over time in tumor biology may not be well represented by a single metastatic biopsy (5, 6). It is in this context that the assessment of genomic alterations in circulating tumor cells (CTCs) may provide distinct advantages due to the noninvasive method of collection and the ability to perform longitudinal CTC sample collection. Recent data suggest that genomic biomarkers within CTCs, such as AR splice variants (AR-V7), are highly associated with resistance to the commonly-used hormonal therapies enzalutamide or abiraterone acetate (8). Thus, CTCs can provide a potentially clinically useful noninvasive biomarker and source of tumor tissue for tumor biology assessment over time to help facilitate therapy decisions.

To date, CTCs have been largely utilized for enumeration from peripheral blood of patients with mCRPC and used simply for

[1]Department of Medicine, Division of Medical Oncology, Duke Cancer Institute, Duke University Medical Center, Durham, North Carolina. [2]Duke Molecular Physiology Institute, Duke University, Durham, North Carolina. [3]Wake Forest School of Medicine, Winston Salem, North Carolina.

Note: Supplementary data for this article are available at Clinical Cancer Research Online (http://clincancerres.aacrjournals.org/).

Corresponding Author: Andrew J. Armstrong, Divisions of Medical Oncology and Urology, Duke Cancer Institute, Duke University, DUMC Box 103861, Durham NC 27710. Phone: 919-668-8797; Fax 919-660-0178; E-mail: andrew.armstrong@duke.edu

doi: 10.1158/1078-0432.CCR-16-1211

Translational Relevance

We evaluated a method to isolate and genomically characterize circulating tumor cells from men with abiraterone- or enzalutamide-resistant metastatic castration-resistant prostate cancer. In this study, we identified common and reproducible regions of amplification of expected genes such as *AR* and *FOXA1* and losses of *PTEN*, and provide a broad clinically annotated analysis of whole genomic copy gains and losses in this treatment resistance setting. Surprisingly, we found common amplifications of potentially actionable genomic loci containing *ERG* and *BRD4*, as well as acquired gains in *SPOP* and *MYCN*, suggesting additional AR-independent pathways of resistance in this setting. CTC genomic characterization has the potential to provide a minimally invasive predictive biomarker assessment for predicting therapeutic efficacy and broad genomic monitoring for emergent treatment resistance. These findings have clear implications for informative biomarker assessments of AR-directed therapy and taxane resistance but also for novel target discovery and therapeutic development.

prognostication for overall survival, before or during systemic therapy (9). However, the clinical utility of CTCs likely rests in their ability to disclose meaningful predictive biologic information about a cancer that may help select for specific therapies to improve upon outcomes for patients (10).

Only a few pilot studies have assessed whole genomic information from CTCs in men with metastatic prostate cancer. One pilot study assessed CTCs of nine patients with mCRPC using array-based comparative genomic hybridization (aCGH) and identified commonly-gained or lost genomic regions such as *AR* gain or *8q* loss (11). In a comprehensive study of two men with mCRPC, whole exome sequencing of individual CTCs revealed a complex clonally-divergent evolutionary picture in which the majority of truncal mutations from the primary tumor tissue were present in CTCs (12). Finally, a recent RNA sequencing study of 13 patients with mCRPC identified clonal heterogeneity of CTCs within patients and perturbation of several key pathways implicated in CRPC progression, including WNT and AR signaling (13). Thus, there remains a need for additional clinically-annotated whole genomic DNA analysis of CTCs, particularly in the context of contemporary treatment and the development of resistance to enzalutamide or abiraterone acetate. Given that recent data suggest that gains in *AR* are strongly associated with abiraterone resistance in cell-free tumor DNA (14), evaluating copy number changes involving both *AR* and non-AR genomic regions may help identify suitable targets for therapy in the future.

We conducted a prospective study of whole genomic copy number alterations in CTCs from men with mCRPC undergoing therapy with either abiraterone acetate or enzalutamide to better understand the genomic complexities within CTCs that may be feasibly and reliably assessed over time and that may be associated with resistance to systemic therapy.

Materials and Methods

Cell lines, patients, and clinical specimens

Men with progressive, mCRPC were enrolled prior to initiating a new systemic therapy. Eligibility criteria included histologically confirmed adenocarcinoma of the prostate, clinical/radiographic evidence of metastatic disease, castrate levels of testosterone ($\leq$50 ng/dL), and evidence of disease progression on recent CT or bone scan imaging or by consecutive prostate-specific antigen (PSA) rises. We used PCWG2 criteria for PSA rise to determine eligibility for this study (15). Radiographic or symptomatic progression was also permitted as a method to determine eligibility of progression. All men had castrate levels of testosterone. All the mCRPC patients provided informed consent under a protocol approved by the Duke University Institutional Review Board (IRB). Exclusion criteria were limited to the recent receipt of an anthracycline or mitoxantrone within one week of CTC collection given the interfering properties of these agents with CTC autofluorescence and CellSearch-based CTC enumeration. Enzalutamide or abiraterone were used at standard FDA approved doses per standard of care practice. LNCaP and T47D cells were obtained from the Duke University Cell Culture Facility Shared Resource, which authenticates cell lines by short tandem repeat profiling prior to freezing. Subsequent to reanimation, cells were cultured at 37°C and 5% CO_2 in RPMI supplemented with 10% FBS and 1% penicillin and streptomycin for fewer than five passages prior to the extraction of genomic DNA.

CTC enumeration and whole genome amplification

CTCs were enumerated using the standard CellSearch method (9) with samples processed within 48 hours of collection. Blood was also collected in a separate 10-mL ethylenediaminetetraacetic acid (EDTA) tube for CTC genomic analysis. After ammonium chloride (Gibco, A10492) red cell lysis (1:10 dilution over 10 minutes at room temperature), cells were resuspended in 2 mL of buffer (PBS/-Ca, -Mg, 0.1% BSA, 2 mmol/L EDTA) and depleted of CD45 using anti-CD45–labeled magnetic Dynabeads (Invitrogen, 11153D). After magnetic separation, centrifugation, and blocking for 60 minutes in the dark on ice (10% goat serum in PBS), cells were stained with an anti-EpCAM antibody (AbD Serotek, CMA1870g) labeled with Alexa Mouse IgG1-647 (Invitrogen, Z25008) and anti-Hu CD45-488 (Leinco, C1620), then washed with PBS, and adjusted to a final volume of 500 μL. The nonmagnetized supernatant was resuspended for further CTC isolation using FACS (BD-FACSDiva sorter). CTCs were isolated in a FACS cell sorter using Alexa Fluor–labeled anti-EpCAM and CD45 antibody selection.

Leukocytes ($CD45^+$ cells) were collected as germline control during blood collection and analysis, and CTCs (defined as $EpCAM^+$, $CD45^-$ cells) were collected for somatic genomic analysis at the same time point at disease progression. Gating thresholds for EpCAM and CD45 were selected on the basis of healthy volunteer blood and spiked EpCAM-positive control cells. EpCAM-positive, CD45-negative cells from patient samples or spiked control samples were sorted in 100-μL water to retain the maximum amount of CTCs from the sort. In parallel, buffy coats were isolated from 4 mL of whole blood collected in EDTA tubes, diluted 1:1 with PBS (-Ca, -Mg), and carefully layered on 4 mL of Ficoll-Plaque (GE Healthcare, 17-1440). Cells were centrifuged at $400 \times g$ for 10 minutes at 18°C. Buffy coats were washed with PBS, and centrifuged at $400 \times g$ for 10 minutes at 18°C. Pellets were resuspended in 100 μL of nuclease-free H_2O. The Qiagen RepliGene Single Cell kit and WGA4 kit (Sigma-Aldrich GenomePlex Single Cell Whole Genome Amplification Kit) were used to amplify the DNA from CTCs and buffy coats following the manufacturer's protocols. Amplified gDNA was purified using

the GenElute Gel Extraction Kit (NA1111 SIGMA) and MinElute PCR Purification Kit (Qiagen). The quality and concentration of each amplified gDNA sample was measured in a NanoDrop spectrophotometer. Prior to aCGH analysis, DNA quality and integrity were evaluated by 260/280 ratio and agarose gel electrophoresis, respectively, and stored at −20°C.

aCGH

Before hybridizing the samples on the microarray, the GenomePlex Single Cell Whole Genome Amplification Kit (WGA4) was used to amplify the sample DNA to the yield required for microarray labeling (0.5 μg). Whole genomic amplification and aCGH was performed using Agilent Oligonucleotide Array-Based CGH for Genomic DNA Analysis (G4449A, SurePrint G3 Human CGH array 4×180K) following the manufacturer's protocols. The SurePrint G3 CGH array contains approximately 170,334 Distinct Biological Features, with an approximately 13 Kb overall median CGH probe spacing and approximately 5-10 Mb copy-neutral loss of heterozygosity (LOH) resolution. After washing with buffer 1 and 2, slides were placed in an ozone barrier and scanned using an Agilent Microarray Scanner Type C, which measures fluorescence from two dyes simultaneously (Agilent G2565CA, Duke University Genomics Core Facility). Subsequent to scanning, aCGH .tiff images were uploaded to Agilent CytoGenomics Software for the detection of loss/gain copy-number changes. To limit false positives, stringent filters were applied using a minimum aberration filter as follows: ≥ 3 probes to call an amplification event and an average absolute log ratio for amplification ≥ 0.25 and for loss ≤ -0.25. Furthermore, all genes were also evaluated manually based on probe distribution in a given region within chromosomal aberrations obtained from the CytoGenomics software.

FISH

To assess AR and ERG amplification status in CTCs, CTCs were fixed within the CellSearch cartridge, and a locus-specific probe along with a reference probe were used in FISH assays as described previously (16). This permits visualization of CK^+, $CD45^-$ $DAPI^+$ CTCs for concurrent FISH analysis. For AR, we used 340 kb probes against exon 1. For the TMPRSS2-ERG break apart fusion FISH validation, three probes from repeat chromosome 22 interstitial site BAC clones (RP11-479J1, RP11-383C12, RP11-963N10) were used (17).

Results

Optimization of aCGH

To evaluate the ability of our aCGH method to detect copy number variations (CNVs) in rare cells, we took several approaches. First, we spiked control cancer cell lines with known copy number profiles (T47D cells) into healthy volunteer whole blood and analyzed these cells by aCGH. Pooled $EpCAM^+$ and $CD45^-$ CTCs were isolated for genomic analysis from blood in EDTA tubes through ammonium chloride red blood cell lysis, $CD45^+$ magnetic bead depletion, and flow cytometry sorting as described in the Materials and Methods section (Fig. 1A). In parallel, we amplified genomic (g)DNA from the original unspiked cells and leukocytes. The aCGH workflow (Fig. 1B) was optimized on human female and prostate cancer cell line (LNCaP) gDNA where human male gDNA was used as a reference. In addition, we also performed aCGH from 5 to 200 breast cancer T47D cells spiked into healthy blood and isolated them by immunostaining using EpCAM and CD45 antibodies by FACS. The genomic views of the chromosomal aberrations from human female, spiked LNCaPs, and spiked T47Ds are shown in Supplementary Fig. S1A–S1C, respectively. Importantly, Y-chromosome loss was observed in the female gDNA (Supplementary Fig. S1A). In addition, in concordance with other studies, we identified two commonly-amplified genes in T47D cells, *ERBB2* and *SIX1* in our analysis (Supplementary Fig. S1D; refs. 18, 19). Similarly, we confirmed *PTEN* loss by aCGH in the LNCaP gDNA (Supplementary Fig. S1E). These analyses suggest that our workflow can detect copy number alterations within spiked cells and cell lines from a small number of cells ($\geq$5–10 cells). Indeed, we have also been able to observe both small and large copy alterations in as few as seven cells (patient P37.3, Supplementary Table S1). These analyses provide methodologic validation using control samples and establish the groundwork for patient-based CTC genomic analysis.

Validating aCGH on mCRPC CTCs

Our second approach to validate the aCGH methodology for analysis of CTCs used an assessment of the reproducibility of duplicate pooled CTC samples from patients with mCRPC. We elected to pool CTCs from single blood samples to identify the dominant genomic copy changes in the circulation, recognizing that rare or heterogeneous clones that differ within the CTC population may be missed. In this analysis, we enrolled men with progressive, mCRPC who were starting a new systemic therapy at the Duke Cancer Institute. In this prospective cohort, a total of 29 men with mCRPC contributed blood samples for this study. Seven of 29 (24%) were excluded from the analysis due to undetectable CTCs in the blood. Six additional samples did not pass the quality control screening of genomic DNA. We have previously published on the predictors of CTC detection in the blood of men with mCRPC, finding that men with mCRPC who have one or more poor prognostic factors (liver metastases, pain, high PSA, high alkaline phosphatase, or LDH) are more likely to have detectable CTCs by the CellSearch method. Men with favorable prognosis CRPC are more likely to have undetectable CTCs (20). Thus, based on quantity and quality a total of 16 samples from a total of 12 unique subjects (~72% of the total number of samples with CTCs) where two men had two samples drawn and one man had three samples blood drawn with seven or more CTCs were selected for aCGH analysis (Fig. 1C).

To assess the reproducibility of the whole genomic data from CTCs, we performed duplicate aCGH on samples 36.1 and 37.3 along with matched leukocyte controls from the same patient. As demonstrated in Supplementary Fig. S2Aa, the majority (66%) of genomic aberrations were replicated in the 36.1 duplicate samples using strict genome-level gain/loss calling criteria. We also observed a significant number of genes within chromosomal aberrations (Supplementary Fig. S2Ab), and specifically confirmed *AR (Xq12)* amplification in both replicates (Supplementary Fig. S2Ac). For patient sample 37.3, a dye swapping experiment was performed in which the initial labeling of the CTCs and leukocytes was reversed and analyzed. We found 70% of the genomic aberrations were replicated in sample 37.3 using dye swapping, suggesting that the majority of genomic gains/losses are reproducibly identified with this method (Supplementary Fig. S2Ba and S2Bb). On the basis of these results, using technical replicates, dye swap replicates, and an alternative method to identify *AR* gain, our data suggest that our methods can reliably detect common CNVs in CTCs from men with mCRPC using aCGH.

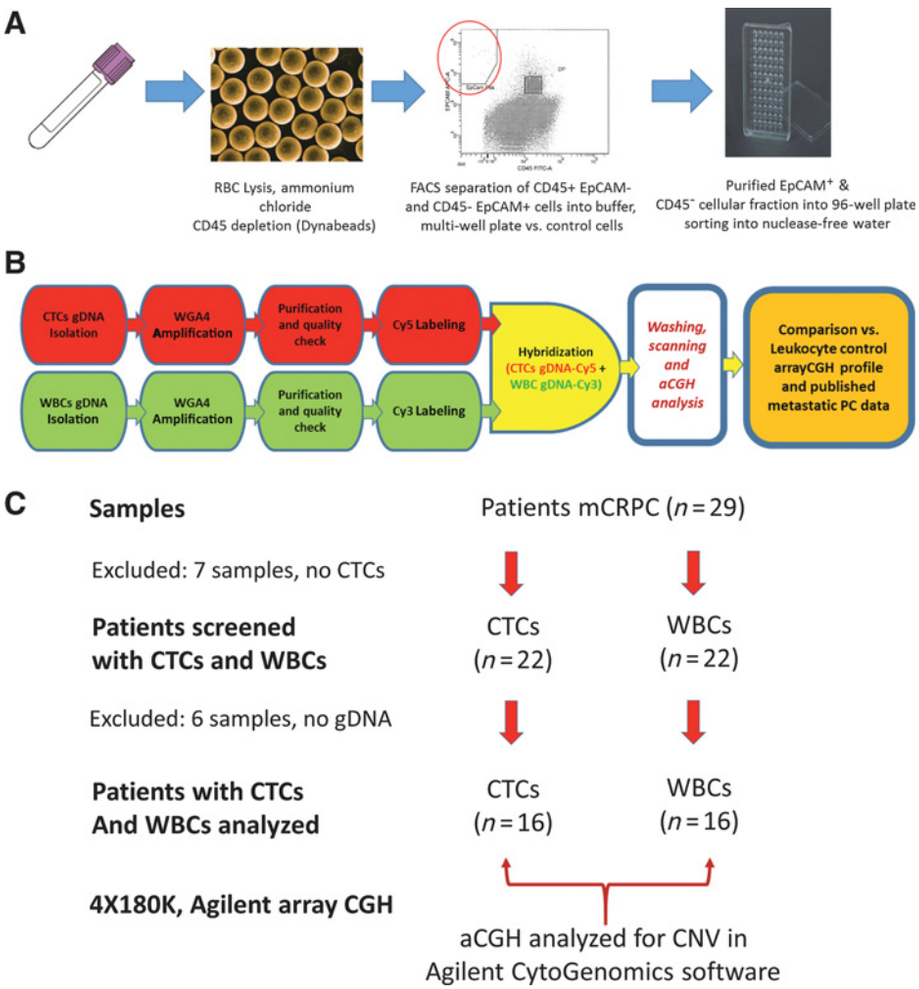

Figure 1.
Methods for the isolation and amplification of genomic (g)DNA from CTCs. **A,** CTCs were isolated from EDTA whole blood after ammonium chloride red blood cell (RBC) lysis, anti-CD45 Dynabead leukocyte depletion, and flow sorting using both EpCAM and CD45 antibodies. $EpCAM^{+}$ and $CD45^{-}$ CTCs were collected in nuclease-free water for genomic DNA (gDNA) amplification, and leukocytes were collected as a germline reference from the same patient. **B,** Workflow of gDNA preparation, purification, hybridization, and aCGH. CTC aCGH results were compared with germline leukocyte control and previously published metastatic prostate cancer data. **C,** CONSORT diagram of CRPC patient samples analyzed in this study. There were two samples where blood was collected at two different time points, and one patient in which blood was collected three times. Sixteen samples had sufficient CTCs (>5) for aCGH analysis.

Genomic profiling of CTCs

After establishing the reliability of our method, we next performed aCGH on gDNA isolated from 12 evaluable men with mCRPC who provided 16 evaluable samples including CTCs and matched reference leukocytes to identify and describe somatically-acquired CNVs in CTCs over time. Patient blood samples were collected before and after progression on enzalutamide or abiraterone acetate therapy and used for CTC isolation and enumeration. Details of these and additional cases are included in Supplementary Table S1 and additional detailed clinical vignettes are provided for six selected men with mCRPC (Fig. 2). All men had mCRPC and progressed on abiraterone acetate, with CTCs drawn for aCGH at progression [blood draw point indicated as an asterisk (*) in Fig. 2]. Three of these men were also enzalutamide resistant (P13, P18, and P40), while two men had a short-term response to enzalutamide after abiraterone (P27, P32), and one had a response to docetaxel chemotherapy followed by progression (P36). Overall, we successfully performed aCGH from CTCs and leukocytes from 16 samples from men with CRPC, including several replicates and one patient (P27) with sequential, longitudinal CTC aCGH. Fig. 5 summarizes the aCGH findings from these men, grouped according to the most common genomic regions altered and by pathway, and compared against reference mCRPC datasets (1, 21).

Our overall findings suggest diverse between-patient heterogeneity in the clonal genomic landscape of CTCs from men with mCRPC (Fig. 5), as well as clonal divergent evolution of CTCs during treatment with abiraterone or enzalutamide. The following three examples illustrate this heterogeneity on a case by case basis. Patient P18 was a man with bone-predominant mCRPC who progressed on abiraterone, and did not respond to enzalutamide. The man developed rapid bone marrow failure and symptomatic progression. His CTCs were characterized by gain of *CYP11A1*, *ERG*, and *BRD4* and loss of *CDK12* and *c-MET*. Patient P13 was a man with bone-only mCRPC who did not respond to enzalutamide after abiraterone and docetaxel chemotherapy. His CTCs were characterized by gain in *MLL2/3*, *FGFR2*, and *ERG* and loss of *MYC*, *RAF1*, and *AURK-A*. Patient P32 progressed on enzalutamide quickly after initial brief response and was then treated with combined enzalutamide and a PI3 kinase inhibitor. He had disease stabilization on this combination but then progressed within five months of therapy initiation. His CTCs were characterized initially by gain of

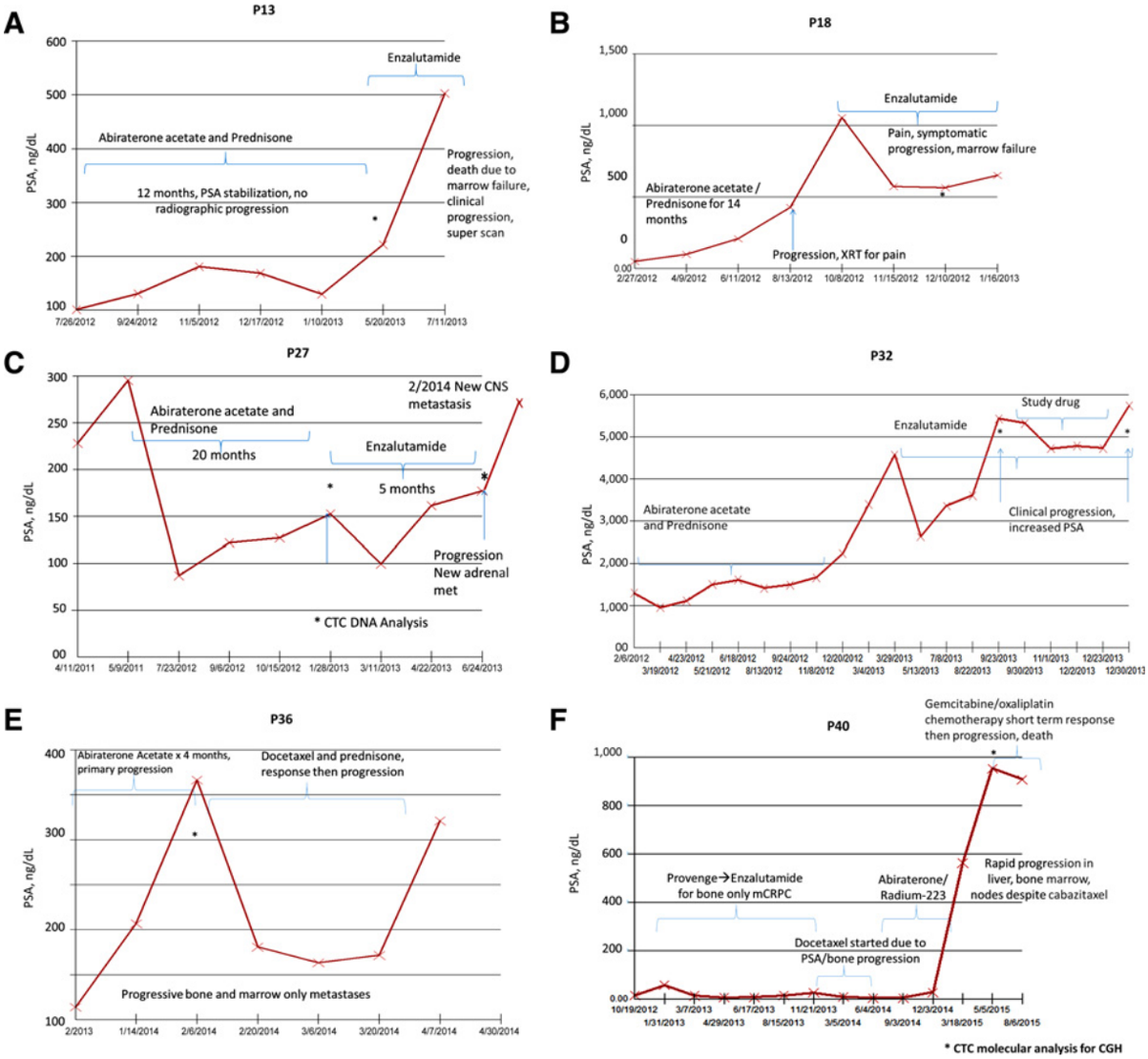

Figure 2.

Case summaries. Clinical course of six selected mCRPC patients (P13, 18, 27, 32, 36, and 40) showing treatments and changes in PSA over time and types of progression. *, time point when CTCs aCGH was analyzed.

SPOP, *AURKA*, *ERG*, and *NCOA2* and loss of *CHD1*. The aCGH results based on these clinical contexts are summarized in Fig. 5.

Overall, we observed *AR* amplification in 50% of CTCs, and loss of the *AR* genomic locus was not observed. We did, however, observe loss of *AR* gain over time. For example, multiple genomic alterations were seen in aCGH analysis of patient P27's CTCs prior to treatment with enzalutamide (Fig. 3A, a), where *AR* gain was observed (Fig. 3A, b), and we confirmed *AR* amplification in this patient using FISH on the same CTCs using an AR-FISH probe, in which four copies of *AR* were found (Fig. 3A, c). However, at the time of visceral progression and enzalutamide resistance, the patient's CTCs lacked this *AR* gain, suggesting clonal selection. In addition, we observed evidence of clonal evolution in this patient. P27 was a man with mCRPC who responded to enzalutamide initially (P27.1), but quickly developed resistance to enzalutamide in about five months (P27.3) accompanied by visceral metastatic progression (adrenal and CNS progression, suggestive of a neuroendocrine-like transformation). Comparative aCGH data from samples P27.1 and P27.3 revealed several new chromosomal aberrations that were only seen in post-enzalutamide–treated samples (P27.3) in comparison with pre-enzalutamide treatment (Fig. 3B), including loss of *AR* amplification. For example, *MYCN* copy number neutrality or modest loss was demonstrated in CTCs collected prior to starting enzalutamide (P27.1), but amplification of the *MYCN* gene locus in CTCs was observed after the patient developed enzalutamide resistance (P27.3; Fig. 3C). *PTEN* gain was also observed in patient 27 pre-enzalutamide (P27.1), with loss after enzalutamide treatment (P27.3; Fig. 3D).

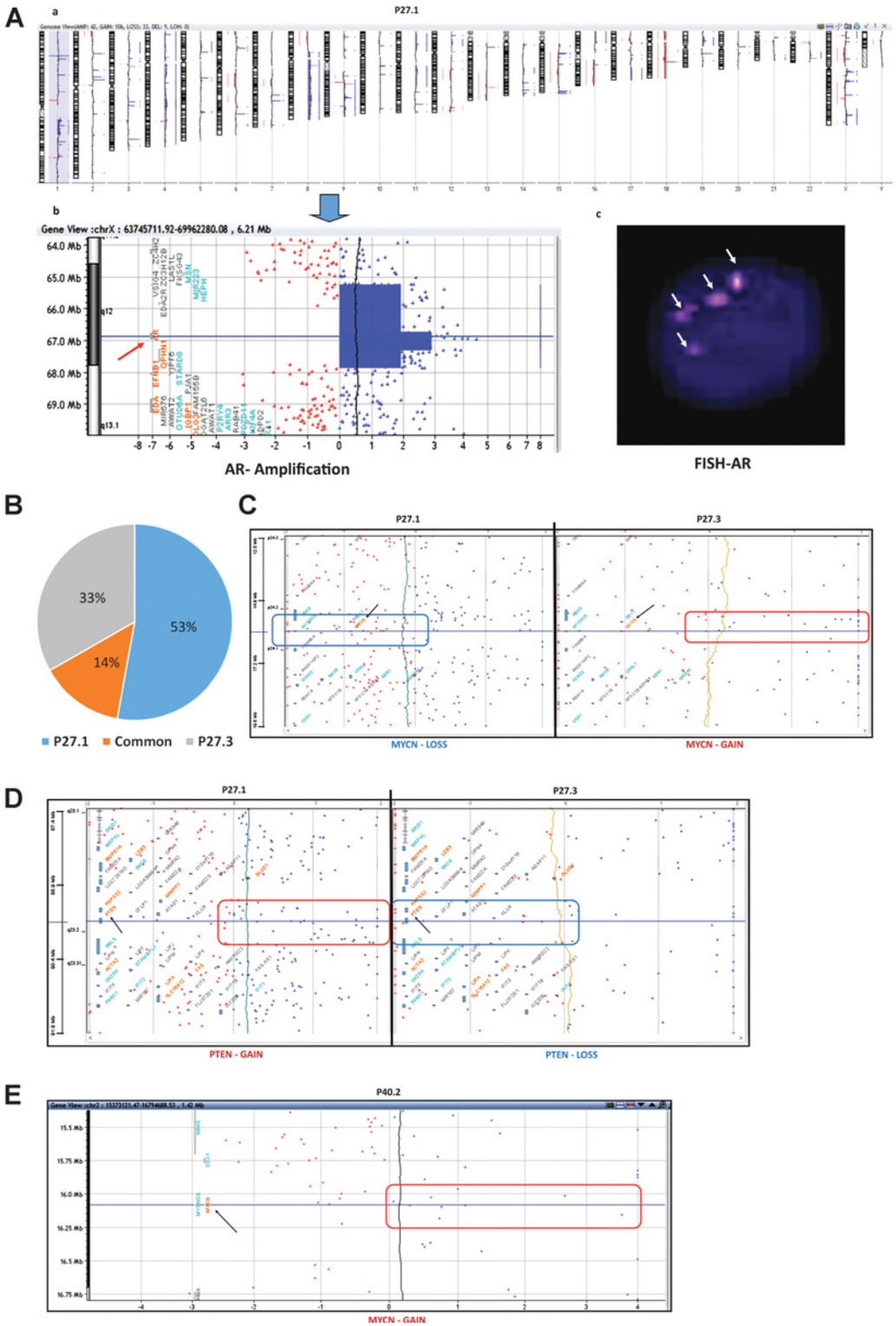

Figure 3.

CTC clonal evolution during enzalutamide therapy. **A, a,** genome view of sample P27.1 (pre-enzalutamide); **b,** aCGH showing *AR* amplification; **c,** validated by FISH using a specific AR FISH probe. Four copies of androgen receptor (AR) are observed. **B,** CTC aCGH prior to enzalutamide (P27.1) and upon progression on enzalutamide (P27.3). Genes with chromosomal aberrations obtained by aCGH from 27.1 and 27.3 were compared using Venny2 software for overlap. **C,** aCGH data depicts *MYCN* loss (chromosome 2) in sample P27.1 and amplification in sample P27.3. **D,** aCGH data showing *PTEN* gain in sample P27.1 and loss in sample P27.3. **E**, *MYCN* amplification is also identified in patient P40.2.

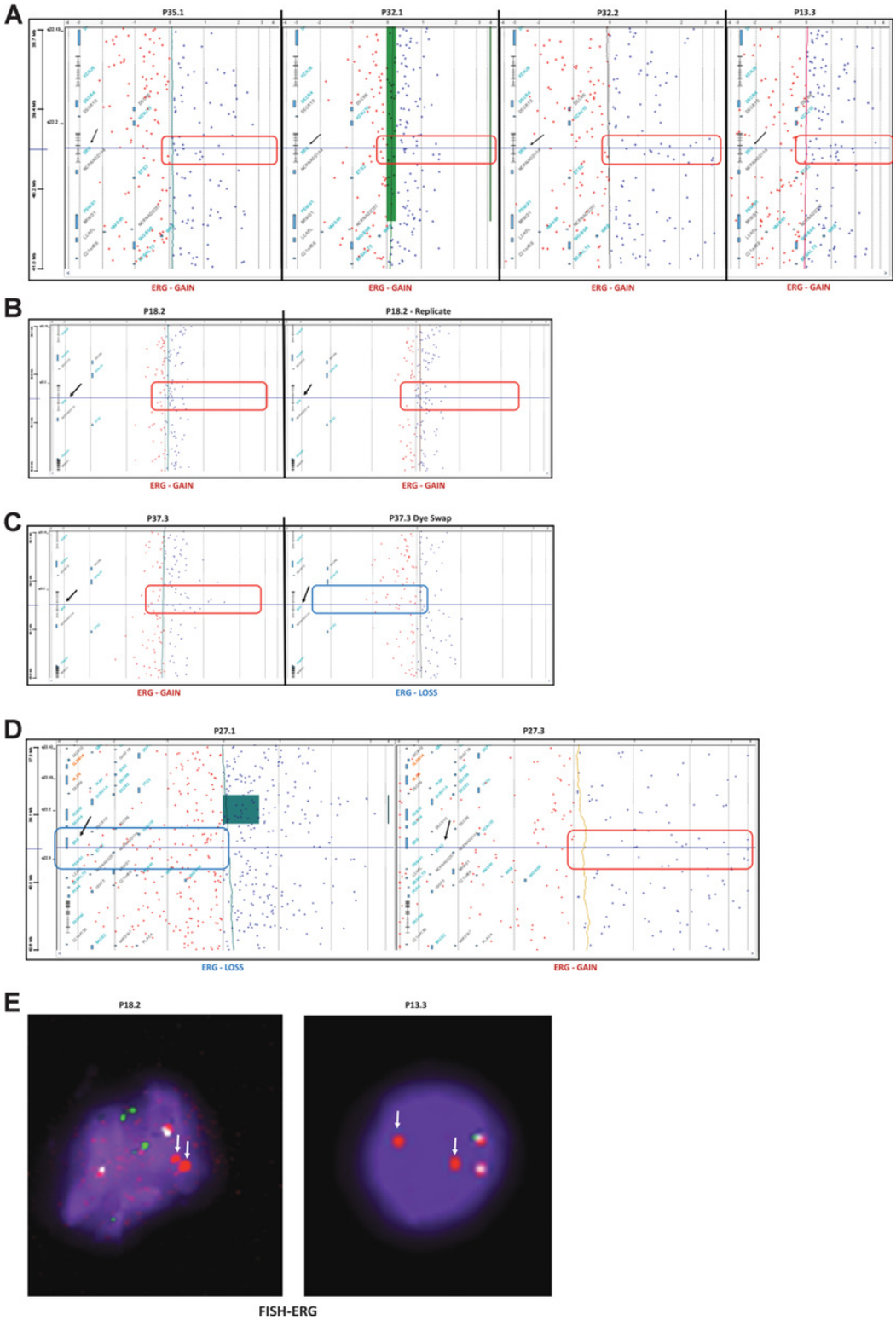

Figure 4.

ERG gain in CTCs from men with mCRPC. aCGH gene view images showing *ERG* gain in; **A,** P35.1, P32.1, P32.2, and P13.3. **B** and **C,** *ERG* gain was observed in both P18.2 and P37.3 and their replicate experiments. For sample P37.3, the replicate sample underwent a dye swap experiment. **D,** Longitudinal sample P27 where *ERG* loss was seen in pre-enzalutamide (P27.1) and gain in post-enzalutamide treatment (P27.3). **E,** Multiple copies of *ERG* are seen in samples P18.2 and 13.3 by the *TMPRSS2-ERG* break apart fusion FISH probe. (*Continued on the following page.*)

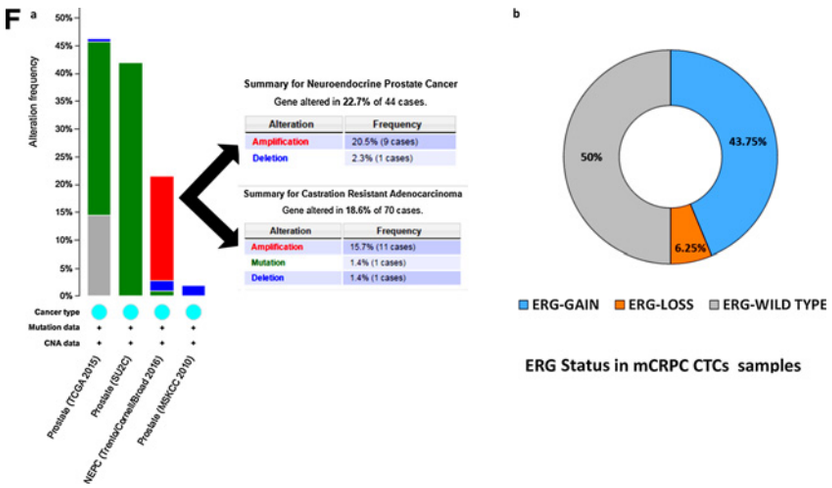

Figure 4.
(*Continued.*) **F, a,** visualization of the prevalence of *ERG* gain across multiple prostate cancer datasets using cBioPortal for Cancer Genomics web-based analysis tool, including our CTC dataset (**b;** pie chart).

MYCN amplification is found in 40% of neuroendocrine prostate cancer (NEPC) cases as compared with just 5% of prostate adenocarcinomas. MYCN induces a neuroendocrine phenotype in prostate cells (22), and has been previously shown to contribute to treatment-induced NEPC after hormonal therapy and resistance to androgen deprivation therapy (ADT). *MYCN* amplification in CTCs was observed in two cases (12.5%). *MYCN* gain was also observed in patient P40.2 (Fig. 3E) as he developed liver metastases following abiraterone, enzalutamide, docetaxel, and radium-223. These data suggest that our CTC aCGH approach can detect the emergence of drug-resistant tumor clones, such as those with gain of the proliferative gene *MYCN*, which corresponded to clinical progression on enzalutamide and visceral spread of their disease.

Patient P13 is a man with *de novo* enzalutamide- and abiraterone-resistant mCRPC whose *AR* was not amplified in his CTCs. This patient was found to have gain of *FGFR2*, *MLL2* and *MLL3*, *PXN*, and *CYP11A*, suggesting additional biologically-relevant pathways in cell signaling, DNA repair, epigenetic control, cell structure, and hormone signaling. Overall, common gains were noted in AR signaling pathways in all 16 males, led by *AR* (50%), *FOXA1* (31.25%), *CYP11B1* (31.25%), and *UGT2B17* (31.25%). Interestingly, the locus encoding the AR coactivator *BRD4* was amplified in 43.75% of CTCs, as was another AR coactivator NCOA2 (ref. 23; Fig. 5). Other known cancer-promoting targets in prostate cancer that were amplified in CTCs from mCRPC patients were Paxillin (*PXN*; 25% gain) and ABL Proto-Oncogene 1 (*ABL1*; 37.5% gain) suggest key roles for these pathways in mediating CRPC progression and drug resistance (Supplementary Fig. S3A–S3G; refs. 24, 25). Patient P32 further illustrates the ability of our CTC aCGH approach to detect genomic evolution over time. P32 is a man with mCRPC, who progressed on enzalutamide and was subsequently treated with the combination of enzalutamide and a PI3K inhibitor, with disease stabilization for five months. His CTCs at progression on the PI3K inhibitor demonstrated *AR* gain and multiple gains of genomic loci containing PI3K-based signaling nodes, while his CTCs at baseline did not have *AR* gain. We analyzed all the AKT and PI3K family members and their regulators listed as part of the Qiagen PI3K-AKT quantitative PCR arrays in SAbiosciences from patient P32.1 and P32.2 CTC aCGH. We found that *AKT2*, *GRB2*, *PIK3R2*, and *PAK1* were gained in both patient P32.1 and P32.2 (Supplementary Fig. S4A). Interestingly, the bruton agammaglobulinemia tyrosine kinase (BTK) gene, used as a biomarker and therapeutic target in prostate cancer (26) was gained in patient P32.1 and lost in P32.2 (Supplementary Fig. S4B). The complex pattern of genomic gains and losses observed in this patient's CTCs suggests clonal selection of CTCs with *AR* gain during combined enzalutamide/PI3K inhibition, concurrent with a PSA rise to over 5,000 ng/dL. His CTCs collected prior to starting the study drug (P32.1) revealed *BRD4*, *ERG*, and *NCOA2* gain, no *AR* copy variation, and *MYCN* loss. These results indicate that clonal selection and dynamic clonal evolution of CTCs may occur during systemic therapy for men with mCRPC, and that reassessment of CTC genomics over time may be informative.

Identification of CTCs harboring *ERG* genomic alterations in mCRPC

The TMPRSS2-ERG fusion is one of the most common recurrent genomic events in more than 50% of men with primary prostate cancer (27). *In vitro*, *in vivo*, and *in silico* studies of ERG have shown its oncogenic activity and association with several oncogenic cancer-promoting pathways in prostate cancer, such as PI3K, Wnt, AR signaling, and glucocorticoid receptor (1, 28). Interestingly, *ERG* duplication/gain has been associated with poor clinical outcome and aggressive disease as compared with patients with a single copy of *ERG* (17). We identified *ERG* gain in 43.75% (7/16) of cases, 6.25% with *ERG* loss (1/16), and 50% (8/16) with wild-type/copy neutral *ERG* (Fig. 4A–D). *ERG* gain was also verified in replicate samples from two independent patients P18.2 and P37.3 (Fig. 4B and C). Interestingly, *ERG* loss was found in sample P27 before enzalutamide treatment (P27.1) and was amplified post-enzalutamide treatment (P27.3;Fig. 4D). We also validated *ERG* amplification in CTCs from patients P18.2 and P13.3 by using the TMPRSS2-ERG FISH probe (Fig. 4E). Next, to compare our findings of *ERG* alteration with public datasets of CRPC samples, we analyzed four different prostate cancer data sets using cBioPortal and found that *ERG* was gained in both CRPC (15.7%) and NEPC (20.5%) clinical samples (Fig. 4F, a; ref. 29). *ERG* copy number alterations from our mCRPC CTCs

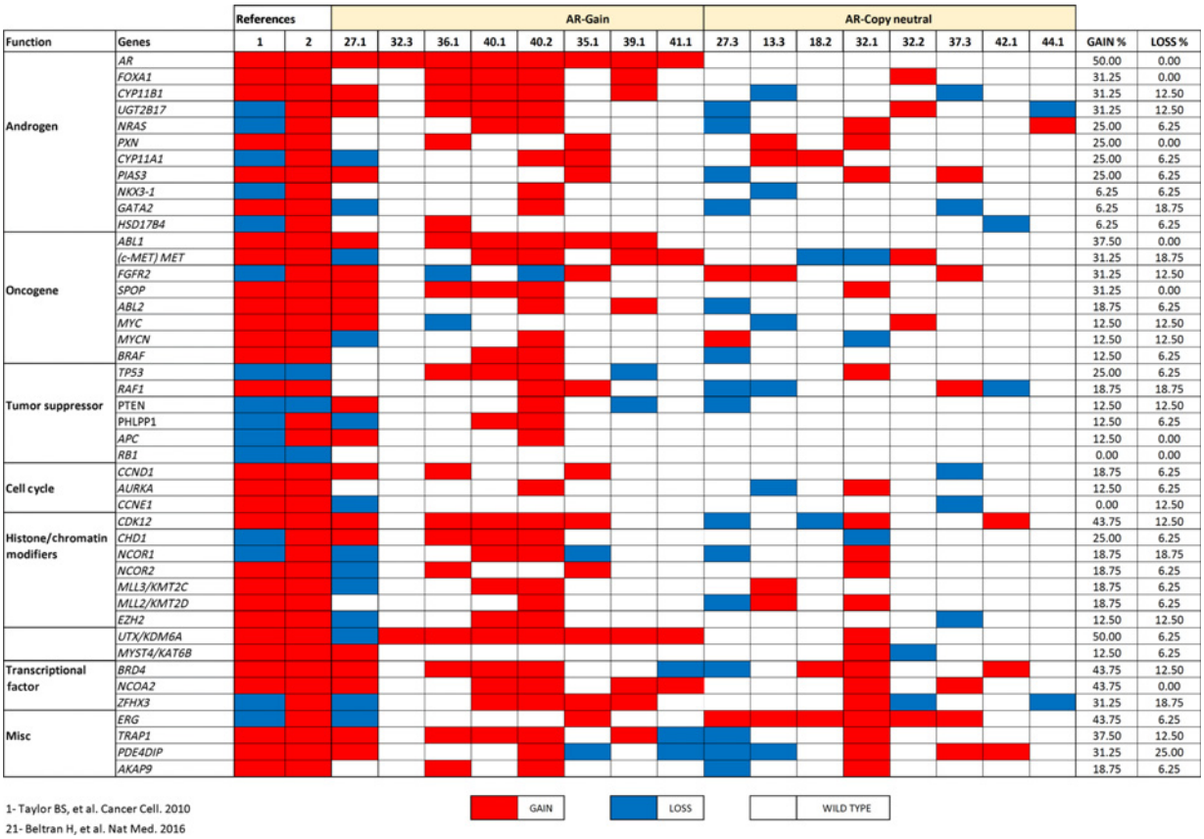

Figure 5.

Summary of copy number alterations observed in CTCs in our study. Subjects are grouped according to their *AR* gain/loss status (top row) and subject IDs (columns). Copy gains (red) and losses (blue), or copy neutral (white) regions in commonly altered genomic regions previously reported in tissue-based metastatic biopsy studies from men with mCRPC are described according to functional categories (rows). Reference data from metastatic biopsies in previous studies are shown on the left side of the table [Column 1- Taylor BS (ref. 1) and column 2- Beltran H (ref. 21)] to provide comparison with these tissue-based datasets. The proportion of patients with CTC gain/loss in a given region is reported on the right.

analysis are shown as a pie chart in Fig. 4F, b. These data suggest a potential enrichment for *ERG* amplification in CTCs from men with mCRPC as compared with localized disease and even metastatic tissue.

Ingenuity pathway analysis

To examine common pathways predicted to be dysregulated in the CTCs of our patients with mCRPC, we performed network and pathway analysis of nonredundant copy number-altered genes from $\geq$ 50% (more than 4 of 7) of cases from either the *AR*-gain or *AR* copy number neutral (wild-type) samples (Fig. 5) using Ingenuity Pathway Analysis (IPA). The copy number-altered genes used for IPA are listed in Supplementary File S1 and S2. IPA results indicated that broad signaling pathways categorized as glucocorticoid biosynthesis, PDGF signaling, pancreatic adenocarcinoma signaling, leukocyte extravasation signaling, ErbB2–ErbB3 signaling, PI3K/AKT signaling, androgen signaling, and prostate cancer signaling were among uniquely-enriched pathways in these mCRPC CTCs with concurrent *AR* gain (Supplementary Table S2), but not in *AR*-copy neutral samples (Supplementary Table S3). Several key genes enriched in the CTCs with *AR* gain have been previously associated with prostate cancer progression, such as MAO (monoamine oxidase)-A (30), CYP11B1, and EBP, which participate in glucocorticoid biosynthesis (31), and the proto-oncogene ABL1 (24). These data suggest that *AR*-amplified tumors may share several addition co-amplified gene sets that contribute to treatment resistance and progression. In the *AR* copy neutral group of CTCs, however, we found no common unifying pathways by IPA using genomic loci of co-amplified or -deleted genomic loci (Supplementary Table S3), suggesting diverse clonality and genomic heterogeneity between patients.

Discussion

Our current genomic study of CTCs from men with mCRPC and abiraterone/enzalutamide resistance demonstrates the feasibility and reliability of aCGH analysis from pooled CTCs in detecting common alterations known to be biologically important in mCRPC. We also demonstrate that this analysis is feasible with low numbers of CTCs down to 7 CTCs/7.5 mL whole blood. From this analysis, we observed common gains in *AR* and *ERG* and losses of *PTEN* as expected. In addition, we identified genomic alterations in chromatin reading (BRD4) and proliferative (MYC,

NMYC) signaling pathways. We also identified significant genomic heterogeneity of CTCs between patients, consistent with prior work from mCRPC tissue samples (32). Importantly, many of these genomic alterations correspond to potentially actionable genomic lesions related to enzalutamide or abiraterone resistance (e.g., ABL amplification, *MYC* and *BRD4* amplification, PI3K pathway alterations). Finally, a novel finding of our study was the identification of *ERG* amplification in CTCs from 40% of our patients. Given recent findings linking ERG expression to taxane resistance, this finding has potential clinical implications for treatment (33). Broadly, our data suggest diverse CTC genomic heterogeneity between patients with mCRPC. This heterogeneity could potentially be missed through single-site metastatic biopsies, and could be obtained through a noninvasive blood test, thus permitting longitudinal analysis.

AR amplification has been reported in a majority of mCRPC samples (1, 2) and has been associated with abiraterone and enzalutamide resistance when detected in cell-free tumor DNA (14, 34). In concordance with this, we also observed *AR* gain in 50% of mCRPC CTC samples. Similarly, NCOA2, an AR coactivator that enhances AR transcriptional activity and signaling resulting in increased prostate cancer progression in early- or late-stage disease, was gained in 20% of primary and 63% of metastatic prostate tumors (1, 35). We detected *NCOA2* amplification in 43.75% of mCRPC CTCs samples. Interestingly, we also observed that 62.5% of AR-positive cases harbor *NCOA2* amplification along with enrichment of androgen and prostate cancer molecular pathways in mCRPC CTCs. These data suggest the common gain of AR-intersecting pathways in CTCs in addition to complex gains and losses in non-AR–based pathways. A novel observation in our CTCs was the relatively common finding of *SPOP* gain in three cases of men with mCRPC and enzalutamide/abiraterone resistance. Recent data suggest that SPOP regulates AR degradation, and this finding suggests a loss of AR pathway dependence in these patients that requires validation in larger studies (36).

ERG rearrangements are a common initiating event in prostate cancer progression, and gain of *ERG* has been previously linked to aggressive variants of prostate cancer (17, 37). In addition, genomic rearrangement of TMPRSS2 and ERG have been shown in multiple studies in both tissues and CTCs, but *ERG* gain/loss has not previously been described in mCRPC tissues or CTCs (27). Our work identified *ERG* gain in 43.75% of CTCs from men with mCRPC, which suggests that this assay may have predictive value for chemotherapy selection given recent links of ERG status with docetaxel sensitivity in men with mCRPC (33).

Additional findings that are noteworthy include our identification of common genomic alterations in epigenetic signaling, DNA repair, and chromatin remodeling pathways, including BRD4, a bromodomain enhancer region implicated in CRPC progression (23). We also observed *KDM6A* gain in 50% and loss in 6.25% cases of mCRPC CTC samples. KDM6A has been shown to play a role in cancer progression in various cancer types, including prostate, breast, pancreatic, head and neck, and esophageal squamous cell carcinoma (38–42). Similarly, Cyclin-Dependent Kinase 12 (CDK12) was amplified in 43.75% and lost in 12.50% of mCRPC cases. Mutations disturbing CDK12 function were identified by others in prostate tumors (43). These data suggest potential biomarkers in individual patients with mCRPC that may be helpful in identifying men who may respond to BRD4, epigenetic, or DNA repair inhibitors, respectively. Finally, FOXA1 (Forkhead-box A1), a transcription factor implicated in AR activation and CRPC progression, was amplified in 31.25% of mCRPC CTC cases without any loss. Increased FOXA1 expression promotes a CRPC-like phenotype and prostate cancer tumor progression. FOXA1 induced tumor cell proliferation in endometrial cancer through the Notch signaling pathway (44–46).

A key observation of our work is the clonal divergence of CTCs during enzalutamide-resistant progression. We observed several instances in which CTCs displayed changes in CNVs prior to therapy and post-therapy, including loss of *AR* gain and gain of *MYCN* during visceral metastatic progression on enzalutamide. These data suggest a clonal selection/evolution during enzalutamide-resistant progression. Tracking the evolution of CNVs in response to therapy within pooled samples of CTCs could help to identify genetic predictive biomarkers and novel treatment targets in mCRPC. Recent work supports this clonal divergent evolution of neuroendocrine-like, non-AR–dependent CRPC during hormonal therapy (21), and our data suggest that this evolution may be noninvasively assessed through CTC analysis.

Limitations of our current work include the small sample size and limited clinical outcomes. However, the present dataset was designed to assess feasibility and generate initial analytic validation for future clinical validation studies, which are ongoing, and is larger than previous studies and adds clinical annotation in the setting of enzalutamide/abiraterone resistance. In addition, there is presently an inability to perform CTC analysis in men without sufficient CTCs, as only 55% of our enrolled men with progressive mCRPC had sufficient CTCs to extract DNA for aCGH analysis. Alternative approaches, such as cell-free DNA and RNA, would be helpful in such cases (47). We report here only copy number analyses, rather than exome or genomic sequencing results, and single base pair mutations or insertions/deletions are missed with this approach. In addition, CTCs may not reflect fully the biology of the primary or metastatic tumors, just as the assessment of a single biopsy may not reflect the heterogeneity of disease within a patient (48). However, our data may be used in concert with sequencing of key targets in CRPC to identify additional single nucleotide variants that may contribute to CRPC progression, such as AR or SPOP mutations (2). Finally, we only evaluated DNA, and thus we did not measure RNA variants, such as AR-V7, which is highly associated with predicted resistance to AR-directed therapies such as enzalutamide or abiraterone (49). Analysis of both mutations and copy changes may yield complementary data of clinical importance, as would analysis of RNA variants such as AR-V7. We are presently conducting a multicenter external and biomarker discovery trial of this and other CTC-based AR-variant assays as well as CTC copy number (particularly *AR* gain) variation and exome mutations in the context of abiraterone and enzalutamide therapy in men with mCRPC (refs. 14, 50; PCF-Movember Challenge trial, clinicaltrial.gov NCT02269982).

In conclusion, we have developed a method for the reliable assessment of broad copy genomic number alterations in CTCs from men with mCRPC that may serve as a noninvasive assessment of clinical pathobiology and predictive medicine. Such an assessment may overcome the need for invasive tumor biopsies in the future to assess such genetic lesions, and provide information that may be missed through single site metastatic or primary tumor biopsies due to the known molecular heterogeneity of CRPC within and between patients (1, 2, 48). Such CTC-based assessments, when ideally coupled with exomic and RNA-based biomarkers, may provide a more comprehensive noninvasive

assessment of the dominant hematogenous metastatic clone at a given point in time and may be assessed repeatedly over time during clonal selection or tumor evolution. Our study highlights that molecular analysis of CTCs should be paired with clinical annotation and outcomes with specific therapies to develop predictive biomarkers of treatment benefit or resistance. For example, given recent associations between *ERG* gain and taxane resistance in CRPC, and *AR* gain and abiraterone resistance, our CTCs aCGH method may permit such future studies using a noninvasive biomarker-driven selection of patients more likely to benefit from such therapies. In addition, our broad platform may allow for the detection of neuroendocrine-based tumor biology, such as *MYCN* amplifications, and other genomic events associated with treatment resistance. Our findings suggest that copy gain/loss-based examination of CTCs could potentially guide standard and future novel treatment options in men with mCRPC. However, this approach requires future prospective studies of specific agents in biomarker-selected patients.

Finally, aCGH enables comprehensive analysis across the genome for discovery of genomic regions that may be missed using a targeted approach of a panel of cancer genes. However, the disadvantage is clearly the costs and complexity of this approach and the enormous amount of data and bioinformatics analysis required to integrate this data for clinical utility. For our purposes of discovery, aCGH was appropriate. In the future, however, specific actionable DNA regions or RNA variants may be preferred for the purposes of specific clinical decision points and selection of therapy, such as AR-V7 and enzalutamide resistance. Our approach identifies a broader and more complex genomic landscape in CTCs than simply measuring AR-V7, however, and highlights the importance of a full molecular characterization for selecting and developing novel strategies across a population of men with mCRPC and at the individual patient level. Overall, our results suggest the potential of the genomic analysis of CTCs to help identify and longitudinally track predictive biomarkers of systemic therapy efficacy and resistance in the clinic.

Disclosure of Potential Conflicts of Interest

A.J. Armstrong reports receiving commercial research grants from Dendreon, Janssen, Medivation, and Sanofi Aventis; speakers bureau honoraria from Dendreon and Sanofi Aventis; and is a consultant/advisory board member for Bayer, Eisai, Janssen, and Medivation. No potential conflicts of interest were disclosed by the other authors.

Authors' Contributions

Conception and design: S. Gupta, J. Li, R.L. Bitting, S. Gregory, A.J. Armstrong
Development of methodology: S. Gupta, J. Li, R.L. Bitting, S. Gregory, A.J. Armstrong
Acquisition of data (provided animals, acquired and managed patients, provided facilities, etc.): S. Gupta, J. Li, G. Kemeny, R.L. Bitting, A.J. Armstrong
Analysis and interpretation of data (e.g., statistical analysis, biostatistics, computational analysis): S. Gupta, J. Li, J. Beaver, J.A. Somarelli, K.E. Ware, S. Gregory, A.J. Armstrong
Writing, review, and/or revision of the manuscript: S. Gupta, J. Li, R.L. Bitting, J.A. Somarelli, K.E. Ware, S. Gregory, A.J. Armstrong
Administrative, technical, or material support (i.e., reporting or organizing data, constructing databases): S. Gupta, S. Gregory, A.J. Armstrong
Study supervision: S. Gupta, A.J. Armstrong

Acknowledgments

We acknowledge support from the Flow Cytometry Shared Resource (FCSR) Duke University, DCI clinical trial infrastructure, Duke University Genomics Core Facility, Duke Cancer Institute, The Duke University Genitourinary Oncology Laboratory, Duke Molecular Physiology Institute core facility, and the Duke University Department of Orthopaedics. We acknowledge Brad Foulk PhD of Janssen Diagnostics for performance of CTC FISH assays.

Grant Support

This work was supported by the Robert B. Goergen Prostate Cancer Foundation Young Investigator Award and the Department of Defense Physician Research Training Award (W81XWH-10-1-0483; to A. Armstrong).

The costs of publication of this article were defrayed in part by the payment of page charges. This article must therefore be hereby marked *advertisement* in accordance with 18 U.S.C. Section 1734 solely to indicate this fact.

Received May 13, 2016; revised July 22, 2016; accepted August 25, 2016; published OnlineFirst September 6, 2016.

References

1. Taylor BS, Schultz N, Hieronymus H, Gopalan A, Xiao Y, Carver BS, et al. Integrative genomic profiling of human prostate cancer. Cancer Cell 2010;18:11–22.
2. Robinson D, Van Allen EM, Wu YM, Schultz N, Lonigro RJ, Mosquera JM, et al. Integrative clinical genomics of advanced prostate cancer. Cell 2015; 161:1215–28.
3. Berger MF, Lawrence MS, Demichelis F, Drier Y, Cibulskis K, Sivachenko AY, et al. The genomic complexity of primary human prostate cancer. Nature 2011;470:214–20.
4. Grasso CS, Wu YM, Robinson DR, Cao X, Dhanasekaran SM, Khan AP, et al. The mutational landscape of lethal castration-resistant prostate cancer. Nature 2012;487:239–43.
5. Burrell RA, Swanton C. Tumour heterogeneity and the evolution of polyclonal drug resistance. Mol Oncol 2014;8:1095–111.
6. McGranahan N, Swanton C. Biological and therapeutic impact of intratumor heterogeneity in cancer evolution. Cancer Cell 2015;27:15–26.
7. Loughran CF, Keeling CR. Seeding of tumour cells following breast biopsy: a literature review. Br J Radiol 2011;84:869–74.
8. Antonarakis ES, Lu C, Wang H, Luber B, Nakazawa M, Roeser JC, et al. AR-V7 and resistance to enzalutamide and abiraterone in prostate cancer. N Engl J Med 2014;371:1028–38.
9. de Bono JS, Scher HI, Montgomery RB, Parker C, Miller MC, Tissing H, et al. Circulating tumor cells predict survival benefit from treatment in metastatic castration-resistant prostate cancer. Clin Cancer Res 2008;14:6302–9.
10. Zhang T, Armstrong AJ. Clinical utility of circulating tumor cells in advanced prostate cancer. Curr Oncol Rep 2016;18:3.
11. Magbanua MJ, Sosa EV, Scott JH, Simko J, Collins C, Pinkel D, et al. Isolation and genomic analysis of circulating tumor cells from castration resistant metastatic prostate cancer. BMC Cancer 2012;12:78.
12. Lohr JG, Adalsteinsson VA, Cibulskis K, Choudhury AD, Rosenberg M, Cruz-Gordillo P, et al. Whole-exome sequencing of circulating tumor cells provides a window into metastatic prostate cancer. Nat Biotechnol 2014; 32:479–84.
13. Miyamoto DT, Zheng Y, Wittner BS, Lee RJ, Zhu H, Broderick KT, et al. RNA-Seq of single prostate CTCs implicates noncanonical Wnt signaling in antiandrogen resistance. Science 2015;349:1351–6.
14. Romanel A, Gasi Tandefelt D, Conteduca V, Jayaram A, Casiraghi N, Wetterskog D, et al. Plasma AR and abiraterone-resistant prostate cancer. Sci Transl Med 2015;7:312re10.
15. Scher HI, Halabi S, Tannock I, Morris M, Sternberg CN, Carducci MA, et al. Design and end points of clinical trials for patients with progressive prostate cancer and castrate levels of testosterone: recommendations of the prostate cancer clinical trials working group. J Clin Oncol 2008;26: 1148–59.
16. Attard G, Swennenhuis JF, Olmos D, Reid AH, Vickers E, A'Hern R, et al. Characterization of ERG, AR and PTEN gene status in circulating tumor cells from patients with castration-resistant prostate cancer. Cancer Res 2009;69:2912–8.

17. Attard G, Clark J, Ambroisine L, Fisher G, Kovacs G, Flohr P, et al. Duplication of the fusion of TMPRSS2 to ERG sequences identifies fatal human prostate cancer. Oncogene 2008;27:253–63.
18. Chavez KJ, Garimella SV, Lipkowitz S. Triple negative breast cancer cell lines: one tool in the search for better treatment of triple negative breast cancer. Breast Dis 2010;32:35–48.
19. Reichenberger KJ, Coletta RD, Schulte AP, Varella-Garcia M, Ford HL. Gene amplification is a mechanism of Six1 overexpression in breast cancer. Cancer Res 2005;65:2668–75.
20. Bitting RL, Healy P, Halabi S, George DJ, Goodin M, Armstrong AJ. Clinical phenotypes associated with circulating tumor cell enumeration in metastatic castration-resistant prostate cancer. Urol Oncol 2015;33:110e1–9.
21. Beltran H, Prandi D, Mosquera JM, Benelli M, Puca L, Cyrta J, et al. Divergent clonal evolution of castration-resistant neuroendocrine prostate cancer. Nat Med 2016;22:298–305.
22. Beltran H, Rickman DS, Park K, Chae SS, Sboner A, MacDonald TY, et al. Molecular characterization of neuroendocrine prostate cancer and identification of new drug targets. Cancer Discov 2011;1:487–95.
23. Asangani IA, Dommeti VL, Wang X, Malik R, Cieslik M, Yang R, et al. Therapeutic targeting of BET bromodomain proteins in castration-resistant prostate cancer. Nature 2014;510:278–82.
24. Greuber EK, Smith-Pearson P, Wang J, Pendergast AM. Role of ABL family kinases in cancer: from leukaemia to solid tumours. Nat Rev Cancer 2013;13:559–71.
25. Sen A, O'Malley K, Wang Z, Raj GV, Defranco DB, Hammes SR. Paxillin regulates androgen- and epidermal growth factor-induced MAPK signaling and cell proliferation in prostate cancer cells. J Biol Chem 2010;285:28787–95.
26. Kokabee L, Wang X, Sevinsky CJ, Wang WL, Cheu L, Chittur SV, et al. Bruton's tyrosine kinase is a potential therapeutic target in prostate cancer. Cancer Biol Ther 2015;16:1604–15.
27. Tomlins SA, Rhodes DR, Perner S, Dhanasekaran SM, Mehra R, Sun XW, et al. Recurrent fusion of TMPRSS2 and ETS transcription factor genes in prostate cancer. Science 2005;310:644–8.
28. Gupta S, Iljin K, Sara H, Mpindi JP, Mirtti T, Vainio P, et al. FZD4 as a mediator of ERG oncogene-induced WNT signaling and epithelial-to-mesenchymal transition in human prostate cancer cells. Cancer Res 2010;70:6735–45.
29. Gao J, Aksoy BA, Dogrusoz U, Dresdner G, Gross B, Sumer SO, et al. Integrative analysis of complex cancer genomics and clinical profiles using the cBioPortal. Sci Signal 2013;6:pl1.
30. Gordon RR, Wu M, Huang CY, Harris WP, Sim HG, Lucas JM, et al. Chemotherapy-induced monoamine oxidase expression in prostate carcinoma functions as a cytoprotective resistance enzyme and associates with clinical outcomes. PLoS One 2014;9:e104271.
31. Liu Y, Smith LI, Huang V, Poon V, Coello A, Olah M, et al. Transcriptional regulation of episodic glucocorticoid secretion. Mol Cell Endocrinol 2013;371:62–70.
32. Chen CL, Mahalingam D, Osmulski P, Jadhav RR, Wang CM, Leach RJ, et al. Single-cell analysis of circulating tumor cells identifies cumulative expression patterns of EMT-related genes in metastatic prostate cancer. Prostate 2013;73:813–26.
33. Galletti G, Matov A, Beltran H, Fontugne J, Miguel Mosquera J, Cheung C, et al. ERG induces taxane resistance in castration-resistant prostate cancer. Nat Commun 2014;5:5548.
34. Azad AA, Volik SV, Wyatt AW, Haegert A, Le Bihan S, Bell RH, et al. Androgen receptor gene aberrations in circulating cell-free DNA: biomarkers of therapeutic resistance in castration-resistant prostate cancer. Clin Cancer Res 2015;21:2315–24.
35. Qin J, Lee HJ, Wu SP, Lin SC, Lanz RB, Creighton CJ, et al. Androgen deprivation-induced NCoA2 promotes metastatic and castration-resistant prostate cancer. J Clin Invest 2014;124:5013–26.
36. Geng C, Rajapakshe K, Shah SS, Shou J, Eedunuri VK, Foley C, et al. Androgen receptor is the key transcriptional mediator of the tumor suppressor SPOP in prostate cancer. Cancer Res 2014;74:5631–43.
37. Demichelis F, Setlur SR, Beroukhim R, Perner S, Korbel JO, Lafargue CJ, et al. Distinct genomic aberrations associated with ERG rearranged prostate cancer. Genes Chromosomes Cancer 2009;48:366–80.
38. Jung SH, Shin S, Kim MS, Baek IP, Lee JY, Lee SH, et al. Genetic progression of high grade prostatic intraepithelial neoplasia to prostate cancer. Eur Urol 2015;69:823–30.
39. Su Y, Subedee A, Bloushtain-Qimron N, Savova V, Krzystanek M, Li L, et al. Somatic cell fusions reveal extensive heterogeneity in basal-like breast cancer. Cell Rep 2015;11:1549–63.
40. Waddell N, Pajic M, Patch AM, Chang DK, Kassahn KS, Bailey P, et al. Whole genomes redefine the mutational landscape of pancreatic cancer. Nature 2015;518:495–501.
41. Martin D, Abba MC, Molinolo AA, Vitale-Cross L, Wang Z, Zaida M, et al. The head and neck cancer cell oncogenome: a platform for the development of precision molecular therapies. Oncotarget 2014;5:8906–23.
42. Gao YB, Chen ZL, Li JG, Hu XD, Shi XJ, Sun ZM, et al. Genetic landscape of esophageal squamous cell carcinoma. Nat Genet 2014;46:1097–102.
43. Cancer Genome Atlas Research Network. The molecular taxonomy of primary prostate cancer. Cell 2015;163:1011–25.
44. Qiu M, Bao W, Wang J, Yang T, He X, Liao Y, et al. FOXA1 promotes tumor cell proliferation through AR involving the Notch pathway in endometrial cancer. BMC Cancer 2014;14:78.
45. Robinson JL, Hickey TE, Warren AY, Vowler SL, Carroll T, Lamb AD, et al. Elevated levels of FOXA1 facilitate androgen receptor chromatin binding resulting in a CRPC-like phenotype. Oncogene 2014;33:5666–74.
46. Imamura Y, Sakamoto S, Endo T, Utsumi T, Fuse M, Suyama T, et al. FOXA1 promotes tumor progression in prostate cancer via the insulin-like growth factor binding protein 3 pathway. PLoS One 2012;7:e42456.
47. Schwarzenbach H, Hoon DS, Pantel K. Cell-free nucleic acids as biomarkers in cancer patients. Nat Rev Cancer 2011;11:426–37.
48. Gundem G, Van Loo P, Kremeyer B, Alexandrov LB, Tubio JM, Papaemmanuil E, et al. The evolutionary history of lethal metastatic prostate cancer. Nature 2015;520:353–7.
49. Scher HI, Lu D, Schreiber NA, Louw J, Graf RP, Vargas HA, et al. Association of AR-V7 on circulating tumor cells as a treatment-specific biomarker with outcomes and survival in castration-resistant prostate cancer. JAMA Oncol 2016;2:1441–9.
50. Scher HI, Heller G, Molina A, Attard G, Danila DC, Jia X, et al. Circulating tumor cell biomarker panel as an individual-level surrogate for survival in metastatic castration-resistant prostate cancer. J Clin Oncol 2015;33:1348–55.